

# Skin color independent assessment of aging using skin autofluorescence

Marten Koetsier<sup>1</sup>, Erfan Nur<sup>2</sup>, Han Chunmao<sup>3</sup>, Helen L. Lutgers<sup>4</sup>,  
Thera P. Links<sup>4</sup>, Andries J. Smit<sup>5</sup>, Gerhard Rakhorst<sup>1</sup>, Reindert  
Graaff<sup>1,4,\*</sup>

<sup>1</sup> Department of BioMedical Engineering, <sup>4</sup> Department of Endocrinology and <sup>5</sup> Department of Medicine, University Medical Center Groningen and University of Groningen, Groningen, The Netherlands

<sup>2</sup> Department of Internal Medicine / Haematology, Academic Medical Centre, University of Amsterdam, Amsterdam, The Netherlands

<sup>3</sup> Second Affiliated Hospital Zhejiang University College of Medicine, Hangzhou, 310009, China

<sup>4</sup> UMCG, BioMedical Engineering, PO-Box 196, 9700 AD Groningen, The Netherlands; phone +31 50 3637427; fax +31 50 3633159

[\\*r.graaff@med.umcg.nl](mailto:r.graaff@med.umcg.nl)

**Abstract:** Skin autofluorescence (AF) for the non-invasive assessment of the amount of accumulated tissue Advanced Glycation Endproducts (AGEs) increases with aging. In subjects with darker skin colors, measurements typically result in lower AF values than in subjects with fair skin colors, e.g. due to selective absorption by skin compounds. Our aim was to provide a new method for calculating skin AF, yielding values that are independent of skin color. The deviation of skin AF of healthy subjects with various darker skin types (N = 99) compared to reference values from Caucasians showed to be a function of various parameters that were derived from reflectance and emission spectra in the UV and visible range (adjusted  $R^2 = 80\%$ ). Validation of the new algorithm, based on these findings, in a separate dataset (N = 141) showed that results of skin AF can now be obtained to assess skin AGEs independently of skin color.

© 2010 Optical Society of America

**OCIS codes:** (170.1610) Clinical applications; (120.3890) Medical optics instrumentation; (170.4580) Optical diagnostics for medicine; (170.6510) Spectroscopy, tissue diagnostics; (300.6280) Spectroscopy, fluorescence and luminescence

---

## References and links

1. R. Meerwaldt, R. Graaff, P. H. N. Oomen, T. P. Links, J. J. Jager, N. L. Alderson, S. R. Thorpe, J. W. Baynes, R. O. B. Gans, and A. J. Smit, "Simple non-invasive assessment of advanced glycation endproduct accumulation," *Diabetologia* **47**, 1324–1330 (2004).
2. R. Meerwaldt, J. W. L. Hartog, R. Graaff, R. J. Huisman, T. P. Links, N. C. den Hollander, S. R. Thorpe, J. W. Baynes, G. Navis, R. O. B. Gans, and A. J. Smit, "Skin autofluorescence, a measure of cumulative metabolic stress and advanced glycation end products, predicts mortality in hemodialysis patients," *J. Am. Soc. Nephrol.* **16**, 3687–3693 (2005).
3. N. C. den Hollander, D. J. Mulder, R. Graaff, S. R. Thorpe, J. W. Baynes, G. P. A. Smit, and A. J. Smit, "Advanced glycation end products and the absence of premature atherosclerosis in glycogen storage disease Ia," *J. Inher. Metab. Dis.* **30**, 916–923 (2007).
4. D. J. Mulder, P. L. van Haelst, S. Gross, K. de Leeuw, J. Bijzet, R. Graaff, R. O. Gans, F. Zijlstra, and A. J. Smit, "Skin autofluorescence is elevated in patients with stable coronary artery disease and is associated with serum levels of neopterin and the soluble receptor for advanced glycation end products," *Atherosclerosis* **197**, 217–223 (2008).

5. H. L. Lutgers, E. G. Gerrits, R. Graaff, T. P. Links, W. J. Sluiter, R. O. Gans, H. J. Bilo, and A. J. Smit, "Skin autofluorescence provides additional information to the UK Prospective Diabetes Study (UKPDS) risk score for the estimation of cardiovascular prognosis in type 2 diabetes mellitus," *Diabetologia* **52**, 789–797 (2009).
6. T. Matsumoto, T. Tsurumoto, H. Baba, M. Osaki, H. Enomoto, A. Yonekura, H. Shindo, and T. Miyata, "Measurement of advanced glycation endproducts in skin of patients with rheumatoid arthritis, osteoarthritis, and dialysis-related spondyloarthropathy using non-invasive methods," *Rheumatol. Int.* **28**, 157–160 (2007).
7. H. Ueno, H. Koyama, S. Tanaka, S. Fukumoto, K. Shinohara, T. Shoji, M. Emoto, H. Tahara, R. Kakiya, T. Tabata, T. Miyata, and Y. Nishizawa, "Skin autofluorescence, a marker for advanced glycation end product accumulation, is associated with arterial stiffness in patients with end-stage renal disease," *Metabolism* **57**, 1452–1457 (2008).
8. M. Monami, C. Lamanna, F. Gori, F. Bartalucci, N. Marchionni, and E. Mannucci, "Skin autofluorescence in type 2 diabetes: beyond blood glucose," *Diabetes Res. Clin. Pract.* **79**, 56–60 (2008).
9. D. J. Mulder, T. van de Water, H. L. Lutgers, R. Graaff, R. O. Gans, F. Zijlstra, and A. J. Smit, "Skin autofluorescence, a novel marker for glycemic and oxidative stress-derived advanced glycation endproducts: an overview of current clinical studies, evidence, and limitations," *Diabetes Technol. Ther.* **8**, 523–535 (2006).
10. N. Kollias and A. H. Baqer, "Absorption mechanisms of human melanin in the visible, 400–720 nm," *J. Invest. Dermatol.* **89**, 384–388 (1987).
11. I. Nishidate, Y. Aizu, and H. Mishina, "Estimation of melanin and hemoglobin in skin tissue using multiple regression analysis aided by Monte Carlo simulation," *J. Biomed. Opt.* **9**, 700–710 (2004).
12. G. Zonios and A. Dimou, "Modeling diffuse reflectance from semi-infinite turbid media: application to the study of skin optical properties," *Opt. Express* **14**, 8661–8674 (2006).
13. J. Sandby-Møller, T. Poulsen, and H. C. Wulf, "Influence of epidermal thickness, pigmentation and redness on skin autofluorescence," *Photochem. Photobiol.* **77**, 616–620 (2003).
14. M. Koetsier, H. L. Lutgers, C. de Jonge, T. P. Links, A. J. Smit, and R. Graaff, "Reference values of skin autofluorescence," *Diabetes Technol. Ther.* **12**, 399–403 (2010).
15. Y. P. Sinichkin, N. Kollias, G. I. Zonios, S. R. Utz, and V. V. Tuchin, "Reflectance and fluorescence spectroscopy of human skin in vivo," in *Handbook of optical biomedical diagnostics*, V. V. Tuchin, ed. (SPIE Press, Bellingham, WA, USA, 2002), chap. 13, pp. 725–785.
16. N. Kollias and A. Baqer, "Spectroscopic characteristics of human melanin in vivo," *J. Invest. Dermatol.* **85**, 38–42 (1985).
17. J. B. Dawson, D. J. Barker, D. J. Ellis, E. Grassam, J. A. Cotterill, G. W. Fisher, and J. W. Feather, "A theoretical and experimental study of light absorption and scattering by in vivo skin," *Phys. Med. Biol.* **25**, 695–709 (1980).
18. W. G. Zijlstra, A. Buursma, and O. W. van Assendelft, *Visible and near infrared absorption spectra of human and animal haemoglobin*, (VSP BV, Zeist, The Netherlands, 2000).
19. J. W. Feather, M. Hajizadeh-Saffar, G. Leslie, and J. B. Dawson, "A portable scanning reflectance spectrophotometer using visible wavelengths for the rapid measurement of skin pigments," *Phys. Med. Biol.* **34**, 807–820 (1989).
20. R. R. Anderson and J. A. Parrish, "The optics of human skin," *J. Invest. Dermatol.* **77**, 13–19 (1981).
21. J. M. Coremans, C. Ince, H. A. Bruining, and G. J. Puppels, "(Semi-)quantitative analysis of reduced nicotinamide adenine dinucleotide fluorescence images of blood-perfused rat heart," *Biophys. J.* **72**, 1849–1860 (1997).
22. G. N. Stamatas, R. B. Estanislao, M. Suero, Z. S. Rivera, J. Li, A. Khaiat, and N. Kollias, "Facial skin fluorescence as a marker of the skin's response to chronic environmental insults and its dependence on age," *Br. J. Dermatol.* **154**, 125–132 (2006).
23. L. Bachmann, D. M. Zetzell, A. da Costa Ribeiro, L. Gomes, and A. S. Ito, "Fluorescence spectroscopy of biological tissues—A review," *Appl. Spectrosc. Rev.* **41**, 575–590 (2006).
24. M. Koetsier, H. L. Lutgers, A. J. Smit, T. P. Links, R. de Vries, R. O. B. Gans, G. Rakhorst, and R. Graaff, "Skin autofluorescence for the risk assessment of chronic complications in diabetes: a broad excitation range is sufficient," *Opt. Express* **17**, 509–519 (2009).
25. N. Kollias, G. Zonios, and G. N. Stamatas, "Fluorescence spectroscopy of skin," *Vib. Spectrosc.* **28**, 17–23 (2002).
26. G. Zonios, A. Dimou, I. Bassukas, D. Galaris, A. Tsolakidis, and E. Kaxiras, "Melanin absorption spectroscopy: new method for noninvasive skin investigation and melanoma detection," *J. Biomed. Opt.* **13**, 14017 (2008).
27. S. Alaluf, D. Atkins, K. Barrett, M. Blount, N. Carter, and A. Heath, "Ethnic variation in melanin content and composition in photoexposed and photoprotected human skin," *Pigment Cell Res.* **15**, 112–118 (2002).
28. G. S. Barsh, "What controls variation in human skin color?" *PLoS Biol.* **1**, 19–22 (2003).
29. G. Zonios and A. Dimou, "Melanin optical properties provide evidence for chemical and structural disorder in vivo," *Opt. Express* **16**, 8263–8268 (2008).
30. R. Na, I.-M. Stender, M. Henriksen, and H. C. Wulf, "Autofluorescence of human skin is age-related after correction for skin pigmentation and redness," *J. Invest. Dermatol.* **116**, 536–540 (2001).
31. C. Magnain, M. Elias, and J.-M. Frigerio, "Skin color modeling using the radiative transfer equation solved by the auxiliary function method," *J. Opt. Soc. Am. A.* **24**, 2196–2205 (2007).
32. K. P. Nielsen, L. Zhao, G. A. Ryzhikov, M. S. Biryulina, E. R. Sommersten, J. J. Stamnes, K. Stamnes, and J. Moan, "Retrieval of the physiological state of human skin from UV–Vis reflectance spectra – a feasibility

- study," J. Photochem. Photobiol. B. **93**, 23–31 (2008).
33. K. M. Katika and L. Pilon, "Steady-state directional diffuse reflectance and fluorescence of human skin," Appl. Opt. **45**, 4174–4183 (2006).
  34. R. Chen, Z. Huang, H. Lui, I. Hamzavi, D. I. McLean, S. Xie, and H. Zeng, "Monte Carlo simulation of cutaneous reflectance and fluorescence measurements – The effect of melanin contents and localization," J. Photochem. Photobiol. B. **86**, 219–226 (2007).
- 

## 1. Introduction

Measuring skin autofluorescence (*AF*) is a non-invasive method for determining the amount of accumulated tissue Advanced Glycation Endproducts (AGEs). A significant correlation exists between skin *AF* and levels of skin AGEs like pentosidine, N<sup>ε</sup>-carboxy-methyllysine (CML) and N<sup>ε</sup>-carboxy-ethyllysine (CEL), as obtained from skin biopsies: in a combined analysis of skin biopsy validation studies, [Koetsier 2010] 76% of the variation in skin *AF* can be explained by variations in skin biopsy pentosidine levels [1–3]. Skin *AF* has shown to increase with age and is also an independent predictor of development and progression of complications in diabetes mellitus, renal failure and other diseases with increased cardiovascular risk [2, 4–8]. Skin *AF* is measured with the AGE Reader, from the mean emission in the 420 – 600 nm range upon UV-A excitation with a peak wavelength of 370 nm.

Skin *AF* measurements in subjects with darker skin colors (UV-reflectance below 10%) typically result in lower values than in subjects with fair skin colors [9]. It is not expected that these subjects have a substantially lower amount of AGEs. The lower *AF* values are therefore expected to be caused by different absorption of excitation or emission light by skin compounds and scattering effects, especially in the epidermis, and specular reflectance. The observed skin color dependence hinders reliable assessment of skin AGEs in subjects with darker skin color and inhibits the recognition of increased skin *AF* values.

Although literature provides some methods to describe the influence of absorbers and scatterers on skin color [10–13], for the current study, we have chosen for an empirical approach by using parameters that are calculated from spectra that are measured individually in the UV-A and visible range (350 – 675 nm). The focus was to develop a model to adapt skin *AF* in healthy subjects for the influence of skin color. For this model, the main spectral characteristics of the strongest contributing absorbers, melanin, hemoglobin and bilirubin, have been used as a basis for finding significant parameters that may describe the lower skin *AF* values in subjects with a dark skin color.

In the current study, various parameters from the spectra are described, that may correlate with the decrease of *AF* for darker skin colors. With these parameters, multiple linear regression analysis was performed to find a model to describe the deviation of *AF* from an expected value. Based on this model, an algorithm to calculate skin *AF* has been constructed and subsequently validated using measurements on healthy subjects of various skin color.

## 2. Materials and methods

### 2.1. Measurement setup

Skin *AF* was measured with the AGE Reader (DiagnOptics Technologies BV, Groningen, The Netherlands). A UV-A blacklight tube (F4T5BLB, Philips, Eindhoven, The Netherlands), with a peak wavelength of 370 nm is used to illuminate a ~ 4 cm<sup>2</sup> of the skin on the volar side of the forearm. A spectrum of the light source is shown in Figure 1. A non-contact optical fiber (200 μm diameter) detects the emission and reflected excitation light from ~ 0.4 cm<sup>2</sup> at an angle of 45°. Using a spectrometer (AvaSpec\_2048, Avantes, Eerbeek, The Netherlands) and computer software, the intensity spectrum is analyzed. The value of skin *AF* is calculated as the ratio between the total emission intensity (420 – 600 nm) and the total excitation intensity

(300 – 420 nm), multiplied by 100 and is expressed in arbitrary units. Besides the skin *AF* measurement, UV-reflectance is calculated as the sum of the intensities of the reflected light from the skin in the range 300 – 420 nm, divided by the sum of intensities in the same range from a white reference standard, which is embedded in the AGE Reader and has been calibrated *in situ* against an external reflectance standard. Moreover, a complete diffuse reflectance spectrum is obtained, using a white LED as illumination source in the visible range. This LED is located directly under the detecting fiber. The spectrum of the LED is also shown in Figure 1. All spectra were corrected for dark current and stored in a file for later analysis.

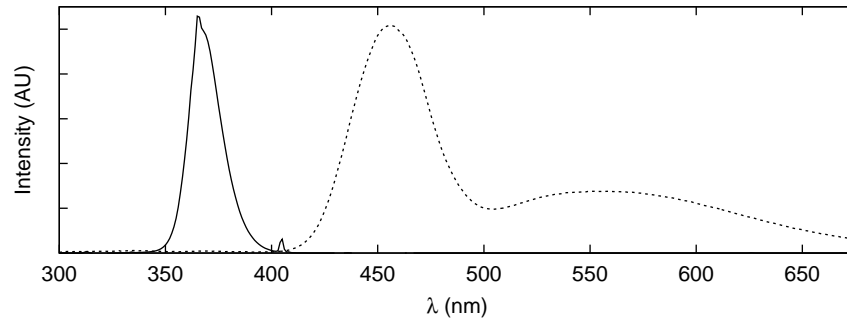


Fig. 1. Spectra of the UV blacklight tube (solid line) and the white LED (dashed line) as used in the AGE Reader. The LED spectrum was magnified to fit on the same scale as the spectrum of the UV tube.

## 2.2. Subjects

Three cohorts of healthy subjects were used in this study. The first group consisted of 61 subjects of Afro-Caribbean descent with a negroid dark skin color, living in the Netherlands. The second group was a group of 120 southern Chinese subjects with intermediate skin color, living in China. The third group consisted of 60 subjects of Asian and African descent, all living in the Netherlands. Health status was obtained by clinical assessment (first and second cohorts) or using a self-administered questionnaire (third cohort). For all these cohorts, only subjects with a UV-reflectance below 12% and with subject age between 20 and 70 years were included. Subjects were excluded if not all spectra were obtained correctly.

For assessing correlations between age-corrected skin *AF* and various parameters that were derived from reflectance spectra in the UV-A and visible range, a subset of 99 subjects (33 subjects from each cohort) was chosen from the total group. The selection focused on obtaining a group of subjects over the full range of age (20 – 70 years) and UV-reflectance values (~ 3% – 12%), and was otherwise random. For the validation, all other subjects were used (N = 142).

## 2.3. Acquiring model parameters

The new algorithm has been based on a model that describes the deviation of the measured *AF* from an expected value. The expected *AF* of an individual can be described as a function of subject age in years, with  $AF = 0.024age + 0.83$ . This relation is based on a large set of Caucasian healthy persons with a UV-reflectance value above 10% [14]. With this, the deviation of skin *AF* for a particular individual is calculated as

$$\Delta AF = AF_m - AF(age) = AF_m - 0.024age - 0.83, \quad (1)$$

where  $AF_m$  is the skin  $AF$  as measured.  $\Delta AF$  was used as the dependent variable in the fitting model.

The next step was finding parameters that describe the skin color and can be measured with the AGE Reader. For this, two types of spectra are available. First, the spectrum that is measured directly from the skin during illumination with the UV light source. This spectrum includes a large peak of UV light that is reflected from the skin and a small emission peak, due to autofluorescence of the AGEs and possibly also other skin compounds with fluorescence emission in the same wavelength region, such as NADH and lipofuscins. Secondly, a reflectance spectrum is available that represents the relative skin reflectance as compared to a white reference standard. This spectrum consists of two parts, one measured with the UV light source,  $\sim 350 - 410$  nm, and one measured with a white light source,  $\sim 415 - 675$  nm. The parameters were based on literature study and own observations.

It is not known whether the parameters as calculated from the spectra are independent of subject age. Therefore, also subject age was included in the model, to compensate for possible interactions.

The parameters were assessed for normality and collinearity using SPSS (version 16, SPSS Inc., Chicago, IL). Parameters were considered normally distributed if a Kolmogorov–Smirnov test resulted in a p-value above 0.05. Parameters were considered independent if the tolerance level exceeded 0.01. For the backward multivariate analysis, threshold p-values of 0.01 and 0.05 were considered.

#### 2.4. Principle of the algorithm

With the parameters found, a prediction model for  $\Delta AF$  was obtained, using a backward multiple linear regression analysis. Since the average expected  $\Delta AF$  of any group of healthy subjects is assumed to be zero, the predicted  $\Delta AF$ ,  $\Delta AF_{pred}$ , was then used as a correction for  $AF$  as

$$AF_{corr} = AF_m - \Delta AF_{pred}. \quad (2)$$

#### 2.5. Validation

Since the low skin  $AF$  values were first observed in subjects that had a UV-reflectance below 10%, the derived algorithm for calculating skin  $AF$  can be validated by describing skin  $AF$  as a function of the UV-reflectance. For this, age-corrected skin  $AF$ ,  $\Delta AF_{corr} = AF_{corr} - AF(\text{age})$ , is used. Requirements are that  $\Delta AF_{corr}$  should not be dependent on UV-reflectance and mean  $\Delta AF_{corr}$  should be close to zero. Furthermore, the increase of skin  $AF$  values with subject age should match the reference values that were found earlier [14].

### 3. Results

#### 3.1. Subjects

Table 1 summarizes group size, skin color and age characteristics of the three cohorts separately and as a whole, for the model development group and the validation group separately. UV-reflectance was used as a measure of skin color. In the first group (subjects of Afro-Caribbean descent), one subject was excluded because of an artifact in one of the spectra.

#### 3.2. Parameters for prediction of $\Delta AF$

The parameters that may predict the deviation of  $AF$  from an expected value,  $\Delta AF$ , are described below. Most parameters are related to melanin, hemoglobin or bilirubin, since these are the strongest absorbers in the skin. The parameters were analyzed for correlations using the dataset of 99 subjects. Table 2 summarizes the parameters analyzed.

Table 1. Group characteristics of the datasets used.

group <sup>a</sup>	size	UV-reflectance (%)		age (years)	
		mean ± sd	range	mean ± sd	range
Measurements used for model development					
group 1 (AC)	33	4.59 ± 1.36	2.55 – 7.99	41.5 ± 11.5	20 – 69
group 2 (SC)	33	9.16 ± 1.54	6.69 – 11.79	40.4 ± 15.8	21 – 70
group 3 (VO)	33	8.49 ± 2.21	4.13 – 11.53	40.9 ± 12.8	20 – 69
total	99	7.41 ± 2.66	2.55 – 11.79	40.9 ± 13.3	20 – 70
Measurements used for validation					
group 1 (AC)	27	5.32 ± 1.68	3.20 – 10.40	41.6 ± 13.5	20 – 70
group 2 (SC)	87	8.61 ± 1.84	4.30 – 11.55	46.8 ± 11.3	24 – 69
group 3 (VO)	27	9.03 ± 2.23	4.20 – 11.68	33.7 ± 10.4	20 – 58
total	141	8.06 ± 2.31	3.20 – 11.68	43.3 ± 12.6	20 – 70

<sup>a</sup> Groups consisted of Afro-Caribbean (AC) and southern Chinese (SC) subjects and subjects of various origin (VO).

Figure 2 and 3 show typical reflectance and emission spectra of three subjects with values of UV-reflectance of 4.4%, 8.0% and 11.4% respectively. The reflectance spectra show some distinctive features, caused by absorption of melanin, hemoglobin and other chromophores. The intensity of these features varies between subjects and this information is used for the various parameters described below. As expected, the average reflectance of a subject with a dark skin color is lower. Figure 3 shows that the measured emission intensity is lower for subjects with darker skin color as well.

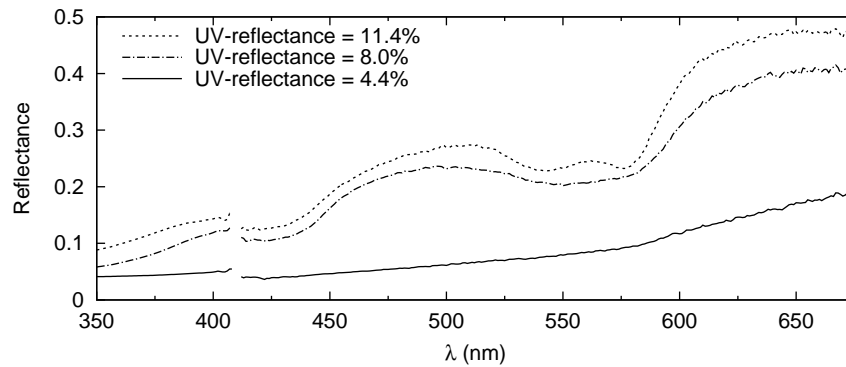


Fig. 2. Typical reflectance spectra of three subjects with varying values of UV-reflectance, showing different intensities of absorption bands. The gap around 410 nm is caused by insufficient intensity of the two light sources (blacklight tube and white LED) in that range. The apparent offset between the reflectance from both light sources is probably due to geometrical differences between the two light sources.



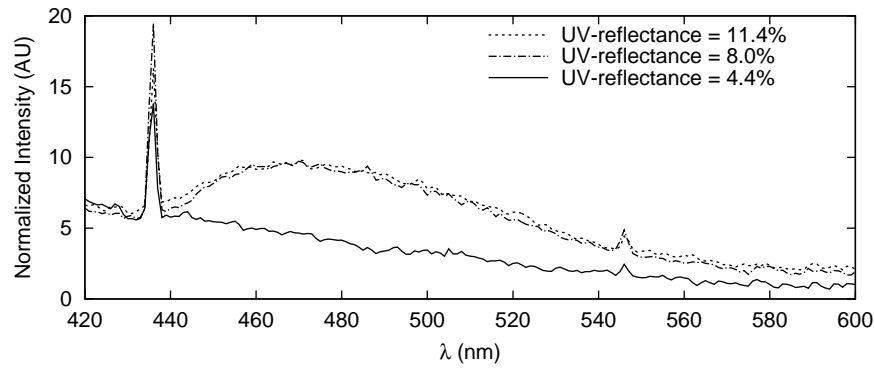


Fig. 3. Typical emission spectra of the same three subjects as shown in Figure 2. The spectra are normalized to the average intensity in the 300 – 420 nm region. The sharp peaks around 436 nm and 546 nm are caused by mercury emission from the UV light source. The subjects with 11.4% and 8.0% UV-reflectance have similar emission peaks, whereas the subject with 4.4% UV-reflectance has a lower emission peak.

### 3.2.1. Reflectance in UV range

Since the start of the development of the AGE Reader, the UV-reflectance has been used as an indication of skin color. With this value, it was found that skin  $AF$  is lower than expected in subjects with darker skin colors [9]. No linear relation could be found with  $\Delta AF$ . Some transformations were analyzed in order to arrive at a linear relation with  $\Delta AF$  and the inverse value of the UV-reflectance ( $InvRefl$ ) was linearly related to  $\Delta AF$ .  $InvRefl$  is used as a parameter in the model, not the UV-reflectance itself.

### 3.2.2. Melanin related parameters

The amount of melanin may be expressed as an index. Sinichkin *et al.* [15] provided three wavelength ranges in which the ratio between the reflectance at two wavelengths (or the slope in a logarithmic spectrum) is used to determine this index.

First, the UV-A wavelength is used, because of the high absorption of melanin in UV. The suggested wavelength range is from 365 – 395 nm. In the AGE Reader, the UV light source is illuminating in this range. However, in our measurements it was found that using 5 nm lower wavelengths yielded a better correlation with  $\Delta AF$ . This wavelength range is centered around the peak wavelength of the light source used. The first melanin index (MI) parameter was defined as

$$MI1 = \frac{R_{390}}{R_{360}}, \quad (3)$$

where  $R$  is reflectance and the subscripts denote the wavelength in nm.

MI may also be derived from the near infrared region, where hemoglobin absorption is relatively small. Kollias and Baqer used wavelengths up to 720 nm [16]. However, the white light source in the AGE Reader does not allow for this range, therefore, wavelengths up to 675 nm were used. Since two references [16, 17] used different starting wavelengths, both pairs 620 – 675 nm and 650 – 675 nm were used in our study:

$$MI2 = 100(OD_{650} - OD_{675}) \quad (4)$$

$$MI3 = 100(OD_{620} - OD_{675}) \quad (5)$$

where  $OD_\lambda$  is the apparent optical density at wavelength  $\lambda$ , defined as  $-\log R_\lambda$ .

Although Sinichkin *et al.* proposed these wavelength pairs as ratios in the OD spectrum, Kollias and Baqer used a regression through the spectrum instead. This method is less prone to artifacts because it does not rely on just two values in the reflectance spectrum. Therefore, we introduced another parameter, *RedLnSlope*, representing the slope of the regression line through the spectrum of  $\ln(R)$  in the range 630 – 675 nm, multiplied by 100.

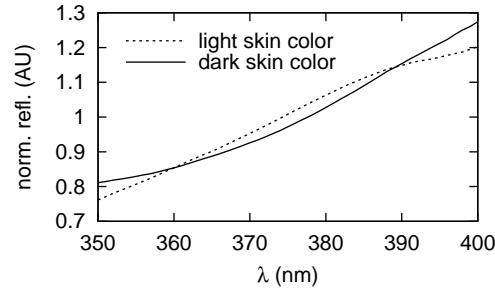


Fig. 4. Reflectance in the UV-A range (in arbitrary units, AU) of subjects with a light skin color and with a dark skin color. The lines represent the average reflectance of six healthy subjects with UV-reflectance of approximately 18% or 6% respectively. For comparison of the shapes, both spectra have been normalized such that average reflectance in the 350 – 400 nm range is 1. Subjects with a light skin color have a convex reflectance spectrum, subjects with a dark skin color have a concave reflectance spectrum.

With more melanin, the melanin absorption causes a stronger decrease in the total reflectance spectrum, especially in the UV-range where melanin is the most important absorber. Figure 4 shows part of the normalized reflectance spectra as measured with the AGE Reader from healthy subjects with light and dark skin color. Both lines represent the average reflectance from six subjects, which were selected for having similar UV-reflectance values (approximately 18% for light skin color and approximately 6% for dark skin color). The shape of the spectrum of the subjects with light skin color appeared convex, whereas that of subjects with dark skin color showed to be concave. This shape can be quantified by assuming a line in the spectrum from the reflectance at 360 nm to the reflectance at 390 nm and then observing the deviation of the reflectance at 375 nm from the line. The shape was thus defined as

$$UVshape = \frac{R_{360} + R_{390}}{2R_{375}}. \quad (6)$$

No correlation was found between *UVshape* and  $\Delta AF$  for subjects with darker skin colors ( $R^2 = 0.077$ ). However, a linear correlation was found between *UVshape* and  $R_{390}$ , the reflectance at 390 nm, showing that *UVshape* is indeed dependent on skin color. With this correlation ( $R^2 = 0.35$ ), a deviation was calculated per measurement, as a function of *UVshape* and  $R_{390}$ :

$$dUVshape = UVshape + 0.407R_{390} - 1.036. \quad (7)$$

This deviation value was found to correlate linearly with  $\Delta AF$  and was used as a parameter.

Furthermore, absolute reflectance values may be correlated to  $\Delta AF$ . In order to avoid interaction with hemoglobin, wavelengths had to be used where hemoglobin absorption is relatively low. Although no large differences in oxygen saturation were expected in healthy subjects, influence of oxygen saturation can easily be omitted by using isobestic points, where oxygenated and de-oxygenated hemoglobin have equal absorption.

Reflectance at the hemoglobin absorption minimum and isobestic point around 500 nm was first assessed. A linear correlation with  $\Delta AF$  was found after a logarithmic transformation. The



transformed parameter is referred to as *LnR500*. Finally, *RedRefl* was introduced as the mean reflectance in the 620 – 675 nm range.

### 3.2.3. Hemoglobin related parameters

Erythema is a condition where the apparent influence of hemoglobin in the skin is increased. Sinichkin *et al.* [15] have summarized the mostly used parameters that assess erythema as an index (EI), using reflectance spectra. These indices can be used to describe the influence of hemoglobin on skin *AF* values. Two different methods to describe erythema have been used. The first was based on the area under the spectral curve of the apparent optical density in the 510 – 610 nm range, calculated as

$$EI1 = 100[OD_{560} + 1.5(OD_{545} + OD_{575}) - 2.0(OD_{510} + OD_{610})], \quad (8)$$

where this wavelength range was chosen to include the specific hemoglobin absorption peaks.

The second method was a simplified version based on comparison of the reflectance at a wavelength where hemoglobin absorptivity is high (560 nm) and at a wavelength where hemoglobin absorptivity is low (650 nm) [18]. Erythema index was thus defined as

$$EI2 = 100(OD_{560} - OD_{650}). \quad (9)$$

Both parameters correlated linearly with  $\Delta AF$  and were used in the model.

Although it was not expected that erythema should be different as a function of skin color, it was expected that a combination of erythema index as calculated with the two suggested methods would yield a good estimate of melanin influence, because the simplified *EI2* method ignores the contribution of melanin absorption, while the first method (*EI1*) should be independent of melanin absorption.

Furthermore, Feather *et al.* [19] developed formulas that describe hemoglobin concentration and oxygenation as indices, based on measurements at isobestic points. These indices were included in the model as parameters

$$HI = 100 \left( \frac{OD_{544} - OD_{527.5}}{16.5} - \frac{OD_{573} - OD_{544}}{29} \right) \quad (10)$$

and

$$OI = \frac{5100}{HI} \times \left( \frac{OD_{573} - OD_{558.5}}{14.5} - \frac{OD_{558.5} - OD_{544}}{14.5} \right) + 42. \quad (11)$$

### 3.2.4. Bilirubin related parameters

Bilirubin has an absorption peak around 470 nm, which is within the emission range of the skin *AF* measurement, and has almost no absorption at 500 nm [20]. To assess the possible additional influence of bilirubin absorption, the ratio of the reflectance at 470 and 500 nm was included in the model as bilirubin index:

$$BI = \frac{R_{470}}{R_{500}}. \quad (12)$$

### 3.2.5. Emission related parameters

It was expected that besides the reflectance spectra, also the emission spectra contained information that could be correlated to  $\Delta AF$ . Because absolute intensities are related to fluorophore content, only relative intensities can be used. Ratios of emission intensities at wavelength pairs 470 and 500 nm (*Em1*), 470 and 570 nm (*Em2*) as well as 600 and 650 nm (*Em3*) were included as parameters. The ratio between mean emission in the 470 – 500 nm and 600 – 650 nm ranges was included as parameter *Em4*.

### 3.3. Univariate analyses

In the dataset of 99 subjects, the parameters as described above were assessed for linear correlation with age-corrected  $AF$ ,  $\Delta AF$ . Table 2 summarizes the univariate linear correlation coefficients (expressed as Pearson's  $R^2$ ) that were found for correlations between  $\Delta AF$  and the various parameters. Because all parameters were designed or transformed as such, only linear correlations existed. Normality was assessed using the Kolmogorov–Smirnov test for each parameter. Significance values of normality (p) are also shown in Table 2. It should be noted that not all parameters had a normal distribution.

Table 2. Results from univariate linear correlations. For each parameter in the model, the square of Pearson's coefficient of correlation is presented ( $R^2$ ). Normality is assessed using a one-sample Kolmogorov–Smirnov test. Values of p above 0.05 indicate a normal distribution.

parameter	description <sup>a</sup>	$R^2$	normality (p)
<i>InvRefl</i>	Inverse of reflectance in UV range	0.452	< 0.01
<i>MI1</i>	Ratio of reflectance at 390 and 360 nm	0.701	0.27
<i>MI2</i>	Difference of <i>OD</i> at 650 and 675 nm	0.651	< 0.01
<i>MI3</i>	Difference of <i>OD</i> at 620 and 675 nm	0.676	< 0.01
<i>RedLnSlope</i>	Slope of line through Ln reflectance in 630 – 675 nm	0.681	< 0.01
<i>dUVshape</i>	Deviation of UV reflectance from straight line	0.541	0.65
<i>LnR500</i>	Natural logarithm of reflectance at 500 nm	0.638	< 0.01
<i>RedRefl</i>	Mean reflectance in 620 – 675 nm range	0.564	< 0.01
<i>EI1</i>	Area under curve of apparent <i>OD</i> spectrum in 510 – 610 nm range	0.202	0.65
<i>EI2</i>	Difference of <i>OD</i> at 560 and 650 nm	0.471	0.47
<i>HI</i>	Hb absorption measured at isobestic points	0.174	0.91
<i>OI</i>	Oxygenation index based on ratio single/double absorption peak Hb	0.001	0.04
<i>BI</i>	Ratio of reflectance at 470 and 500 nm	0.080	0.88
<i>Em1</i>	Ratio of emission at 470 and 500 nm	0.029	< 0.01
<i>Em2</i>	Ratio of emission at 470 and 570 nm	0.004	0.20
<i>Em3</i>	Ratio of emission at 600 and 650 nm	0.082	< 0.01
<i>Em4</i>	Ratio of emission in 470 – 500 and 600 – 650 nm ranges	0.115	< 0.01
<i>Age</i>	Subject age	0.105	0.60

<sup>a</sup> *OD* is defined as  $-\log$  reflectance.

### 3.4. Acquisition of the new algorithm

The parameters as described above were used in a backward multiple linear regression analysis to find a model to describe  $\Delta AF$ . When a  $p = 0.05$  threshold was used, four parameters contributed (*dUVshape* and the three parameters as listed in Table 3). The parameter with the lowest relative contribution, *dUVshape*, had a  $\beta$  value less than half of that of the *MI1* and *RedLnSlope* parameters. Herein, the standardized correlation coefficient  $\beta$  represents the contribution of a specific parameter relative to the contribution of others. Adjusted  $R^2$  was 0.814,

not different from the adjusted  $R^2$  level of 0.804 with the three-parameter model with a  $p < 0.01$  threshold level, which is shown in Table 3. If subject age was not included, adjusted  $R^2$  was 0.731.  $\Delta AF$  can thus be described as a linear combination of the parameters in Table 3, and the new algorithm for calculating skin  $AF$  has been based on these parameters.

Collinearity was assessed as well. Although collinearity was found between some parameters, the significant parameters in the model are independent (tolerance above 0.01).

Table 3. Resulting parameters of the multiple regression analysis. The three-parameter model ( $p < 0.01$  threshold) had an adjusted  $R^2$  of 0.804.

parameter	$\beta$	p	collinearity
(constant)		0.007	
<i>MI1</i>	0.406	0.000	0.226
<i>RedLnSlope</i>	-0.463	0.000	0.228
<i>Age</i>	-0.274	0.000	0.977

### 3.5. Validation

Using the algorithm as obtained above, the corrected value of skin  $AF$ ,  $AF_{corr}$ , was calculated using

$$AF_{corr} = AF_m + \alpha_1 MI1 + \alpha_2 RedLnSlope + \alpha_3 Age, \quad (13)$$

where  $AF_m$  is the measured uncorrected skin  $AF$  and  $\alpha_1$  through  $\alpha_3$  are multiplication constants that were derived using the multiple regression analysis. Skin  $AF$  ( $AF_{corr}$ ) and age-adjusted skin  $AF$  ( $\Delta AF_{corr}$ ) were calculated for each individual in the validation-group.  $\Delta AF_{corr}$  was calculated using Eq. (1), using  $AF_{corr}$  instead of  $AF_m$ . This group consisted of 27 subjects from the Afro-Caribbean cohort, 87 subjects from the South Chinese cohort and 27 from the cohort of subjects of various origin. Age-adjusted skin  $AF$  is shown as a function of UV-reflectance values in Figure 5, also comparing the new algorithm (b) and the old method for calculating skin  $AF$  (a). With the new algorithm, the mean standard deviation of  $\Delta AF_{corr}$  as percentage of the skin  $AF$  is 14.8%.

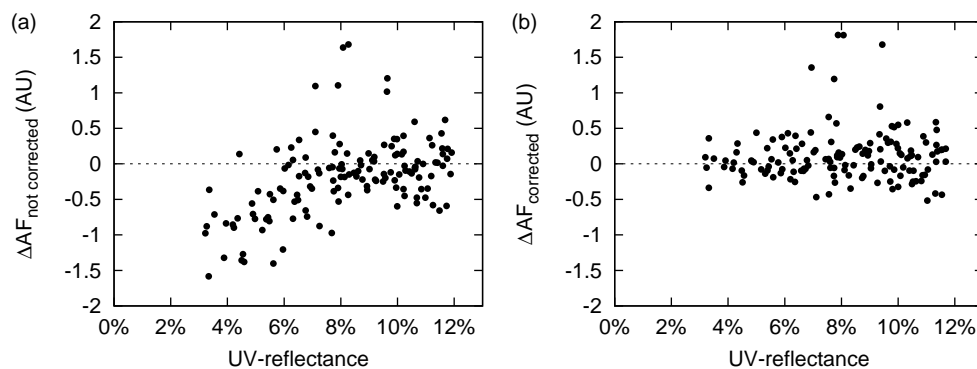


Fig. 5. Age-adjusted skin  $AF$  ( $\Delta AF$ ) as a function of UV-reflectance as calculated without correction for skin color (a) and with the new algorithm (b).

Figure 6 shows the  $AF$  values as a function of subject age, as calculated with the new algorithm (b) as well as without correction for skin color (a). Values are compared with the standard reference line as obtained from Caucasian subjects [14].

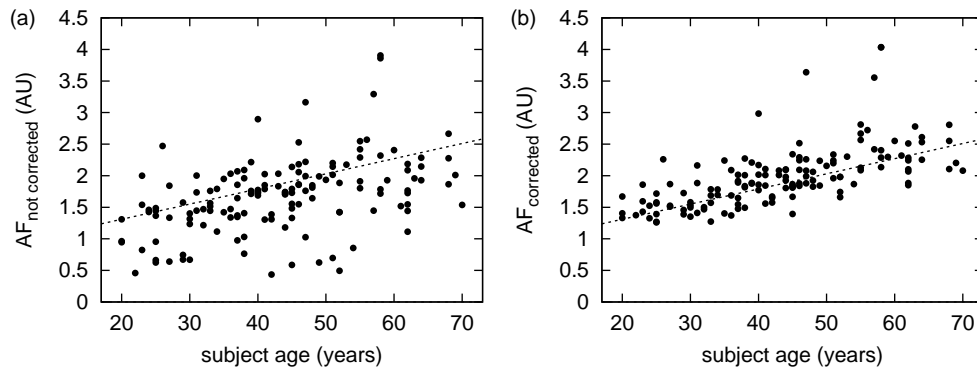


Fig. 6.  $AF$  values as a function of subject age as calculated without correction for skin color (a) and with the new algorithm (b). The dashed line represents the reference values for Caucasian subjects,  $AF = 0.024age + 0.83$  [14].

#### 4. Discussion

The current study describes and validates a new calculation algorithm for skin  $AF$  that enables reliable determination of increased skin  $AF$  in subjects, regardless of the color of the skin. For this algorithm, parameters were applied that were derived from reflectance spectra as measured on the skin that correlate with the originally observed decrease in skin  $AF$  values of subjects with a dark skin color.

To compensate for differences in skin color, skin  $AF$  was initially calculated as the mean light intensity in the emission range divided by the mean light intensity of the light that is reflected from tissue in the excitation range, as suggested previously by Coremans *et al.* [21]. Whenever more melanin or other skin compounds are absorbing emission light, they also absorb more excitation light and by dividing these two quantities, the result will be less dependent on absorption. Using this method, skin  $AF$  can reliably be obtained in subjects with Fitzpatrick skin phototypes I – IV. Stamatatos *et al.* [22] also used the reflectance of the skin as normalization factor for autofluorescence measurements. They also reported that this method is adequate, but only for lighter skin types. In the AGE Reader, a simple skin color assessment is performed using the mean intensity of the UV-A light that is reflected from the skin. It was found that skin  $AF$  can be reliably assessed if more than 10% of the UV-A light is reflected [9, 14]. This method could not compensate for the strong absorption of melanin, as in subjects with a dark skin color.

In the AGE Reader, the excitation light source illuminates in the 350 – 410 nm range and emission is measured in the 420 – 600 nm range. Skin  $AF$  in these ranges may not only be caused by skin AGEs. Also other fluorophores such as keratin, vitamin D, lipofuscin, ceroid, NADH and pyridoxine may add to the total fluorescence signal [23]. Furthermore, some fluorophores have excitation maxima that are within the emission range of the fluorophores above, including porphyrins, elastin crosslinks, FAD, flavins and phospholipids. Due to the overlapping nature of absorption and emission spectra, it is difficult, if not impossible, to assess the influence of specific fluorophores on the total fluorescence signal, especially with the broad excitation peak that is used in the AGE Reader. However, it has been shown that even with this

broad excitation peak, dermal content of specific AGEs explains the major part of the variance (up to 76%) in the skin *AF* signal in a pooled analysis of the validation studies mentioned earlier [1–3], and, moreover, that the risk of chronic complications in diabetes can be assessed [24].

Apart from other fluorophores, non-fluorescent chromophores in the skin may have an effect on skin *AF* by selectively absorbing excitation and/or emission light. The most contributory chromophores in the UV-A and visible region are melanin in the epidermis and hemoglobin in the dermis [15,20,25]. Both in the epidermis and the dermis, also bilirubin and to a lesser extent beta-carotene are present, having absorption peaks at 470 nm and 450 nm respectively [20,23]. Nevertheless, melanin and hemoglobin are widely accepted as the main absorbers.

The absorption spectrum of melanin has been studied extensively *in vitro* [26]. However, melanin resides in the skin in cell organelles, melanosomes, and the effect on skin color and moreover on the measurement of *AF* is influenced by the size, number, distribution and aggregation of these melanosomes in the skin, which may vary largely between individuals of different ethnic groups [27,28]. In general, melanin absorbs light from the UV, visible and near infrared range of the spectrum, with an exponential increase of absorption towards lower wavelengths [26,29].

Hemoglobin has a broad absorption spectrum over the visual part of the spectrum with several absorption peaks and is therefore an important factor in skin color [19,20,23]. Although it is not expected that the hemoglobin concentration or distribution is very different for the various skin phototypes, the apparent optical properties of hemoglobin and their influence on skin *AF* may vary because of interactions with other chromophores (e.g. melanin) during light propagation within the skin. Moreover, hemoglobin is concentrated in red blood cells within blood vessels. Because of a limited and wavelength dependent penetration depth of light in blood vessels, the influence of hemoglobin on skin *AF* is difficult to assess. Nevertheless, Na *et al.* observed a variation of skin autofluorescence in their measurements as a function of skin redness, which depends on hemoglobin concentration or oxygen saturation [30].

Several approaches exist to describe the influence of absorbers and scatterers on skin color. Some methods have used a homogeneous approach [10–13,15], whereas others have defined many layers in the skin, with separate optical properties in each layer, that may vary between subjects [31–34]. Some of these approaches aim at determining the concentration of certain chromophores or identifying specific fluorophores. Since several questions still remain to be solved, the current study has chosen for a more practical approach by using the spectra that are measured individually in the UV-A and visible range (350 – 675 nm), focusing on developing an algorithm to correct skin *AF* in healthy subjects for the influence of skin color, using parameters that are derived from these spectra. For this correction, the main characteristics of only the strongest contributing absorbers, melanin, hemoglobin and bilirubin, have been used as a basis for finding significant spectral properties that may describe the lower skin *AF* values in subjects with a dark skin color. To achieve a simple model, influence of specific fluorophores and less contributory absorbers have not been taken into account.

The developed model, using subject age and two parameters from the reflectance spectrum, could account for over 80% of the relative change in skin *AF* values. The new calculation algorithm, based on this model, yields skin *AF* values that are almost independent of skin color, even without knowing the exact composition of chromophores, fluorophores and scattering particles in the skin.

If a 0.05 threshold was used, the additional *dUVshape* parameter would be included, which had a  $\beta$  value of less than half of that of the other two parameters, *MI1* and *RedLnSlope*. Adjusted  $R^2$  was not better than for the preferred model with only two spectral parameters. Therefore, in this study, the low threshold of 0.01 was chosen for excluding parameters from the model.

In the current study, only age and the *MI1* and *RedLnSlope* parameters of Table 2 were necessary to describe the influence of skin color on skin *AF*. All other parameters, including the parameters from the emission spectra, could be discarded from the final model. A bilirubin related parameter was studied as well because we initially assumed that small changes might also influence the measured skin *AF*. Nevertheless, it should be noted that a significant influence on skin *AF* may be present in conditions such as jaundice. Similarly, the present results can not exclude that strong erythema may also influence skin *AF*.

Subject age is an important predictor for skin *AF* values. Therefore, an age-corrected value, based on reference values of skin *AF* in Caucasian subjects [14], was used in the model. However, the age-dependence of skin *AF* may be different depending on racial or cultural differences, e.g. dietary variations or smoking habits. By applying the same relation of skin *AF* and age to all subjects, equal reference values can be used, allowing the detection of increased skin *AF* independent on skin color. Our results show that corrected *AF* has the same increase with subject age for the entire group of subjects from various descent.

Figure 5 shows some subjects that have higher skin *AF* values as compared to other subjects of the same age, even after correction ( $\Delta AF$  value above 1). We assume that these subjects may have developed an increased cardiovascular risk, without immediate clinical symptoms. It should be noted that in the cohort that was used for developing the model, no increased values of skin *AF* were observed (not shown).

The inclusion of subject age in the model may seem unnecessary at first, because the model was designed to predict  $\Delta AF$ , which reflects a value independent of age. However, it was assumed that age could have an effect on other parameters. Although age did not correlate to any of the parameters, it turned out to be a significant predictor in the model. If age was left out from the model, adjusted  $R^2$  decreased to 0.731.

Although we did not yet attempt to physically explain our observations, the current study suggests that for the purpose of assessing skin AGEs, the influence of skin color on the *AF* measurements may be sufficiently described using age and the *MI1* and *RedLnSlope* parameters, i.e. the ratio of two reflectance values in the 360 – 390 nm range and the slope of the reflectance in the 620 – 675 nm range. This resulted in a mean standard deviation of 14.8% of the *AF* values, which is even lower than the 20% that was observed in a Caucasian group from an earlier study [14]. Therefore, we may have successfully developed a technique to recognize increased values of skin *AF* independent of skin color.

In conclusion, an algorithm to calculate skin *AF* was developed and validated for subjects between 20 and 70 years. With this new method, skin *AF* can now be measured independent of skin color, which makes the measurement of skin *AF* for the non-invasive assessment of increased levels of skin AGEs more generally applicable.

### Competing interest

R. Graaff and A.J. Smit are also founders and stockholders of the university spinoff DiagnOptics Technologies BV, manufacturer of the AGE Reader ([www.diagnoptics.com](http://www.diagnoptics.com)). M. Koetsier is a Ph.D. student at the Department of BioMedical Engineering whose study is partly financed by DiagnOptics Technologies BV.

### Acknowledgements

The authors would like to thank Arthur Buijink of the Academic Medical Center in Amsterdam, The Netherlands, for support with skin *AF* measurements of Afro-Caribbean healthy subjects.